Study of the ELM fluctuation characteristics during the mitigation of type-I ELMs

A V Bogomolov[1], I G J Classen[1], J E Boom[2], A J H Donné[1;3], E Wolfrum[2], W Suttrop[2], N C Luhmann Jr.[4] and the ASDEX Upgrade Team

[1]*FOM-Institute DIFFER, Dutch Institute for Fundamental Energy Research, 3430 BE Nieuwegein, The Netherlands*

[2]*Max-Planck-Institut für Plasmaphysik, Boltzmannstraße 2, 85748 Garching, Germany*

[3]*Eindhoven University of Technology, 5600 MB Eindhoven, The Netherlands* [4]*University of California at Davis, Davis, CA 95616, USA*

Introduction

In the high confinement mode (H-mode) of a tokamak plasma, a magnetohydrodynamic (MHD) instability called the edge localized mode (ELM) appears. These modes expel plasma particles and energy resulting in high power loads on the divertor and, in case of reactor operation can cause intolerable erosion of the first wall materials. Therefore, study of ELMs is needed in order to be able to better control these events in future devices [1].

Several types of ELMs with different properties are known, like type-I ELMs, and small ELMs: type-II ELMs, type-III ELMs and various others. Unlike the most common type-I ELMs, the small ELM regimes are associated with reduced energy losses and, as a consequence, reduced heat flux to the divertor plates [2].

In this paper, the temperature fluctuations associated with ELMs during the transition from type-I to mitigated ('small') ELMs are studied. The main question to be answered is whether the type-I ELMs change their behaviour during the transition, causing them to disappear, or whether the small ELMs become dominant and prevent type-I ELMs from developing.

Electron cyclotron emission imaging (ECEI) is one of the most suitable diagnostics to study ELMs. The ECEI at AUG [3] is a 2D diagnostic which consists of a linear array of 16 detectors, each of which acts as a standard (1D) ECE radiometer. This diagnostic allows the visualization of various MHD instabilities occurring in the plasma with high temporal and spatial resolution.

Experimental set-up

To study the transition from the type-I to the small ELM regime, shot #26081 has been analyzed. The shot has the following parameters: B_t = -2.5 T, I_p = 0.8 MA, P_{NBI} = 7.3 MW and P_{ECRH} = 1.7 MW. The transition to the small ELM regime starts, when the edge density reaches $6 \cdot 10^{19}$ m^{-3}. During the transition phase smaller crashes start to appear in between the type-I ELM crashes, while the type-I ELMs appear less frequently until they totally disappear.

Three different phases of the shot are analyzed: clear type-I ELMs (before 1.4 s), the transition phase from type-I to smaller ELMs (1.4 - 2.7 s), and the phase of mitigated type-I ELMs (2.7 - 5.3 s) where only small ELMs were observed.

Investigation of ELM characteristics: Mode intensity

The type-I ELM crash consists of an ELM onset mode, where relatively coherent temperature fluctuations are seen and the crash itself, where temperature fluctuations become chaotic and result in a drop of plasma temperature. Quantitative evaluation of the intensity of type-I ELM onsets can be obtained by calculating the integral spectral power in the frequency range 10-70 kHz, where the broadband fluctuations occur [4]. Fig. 1 shows ELM synchronized integral spectral power which represent mode amplitudes (for type-I ELM onsets on the left, and for small ELMs on the right).

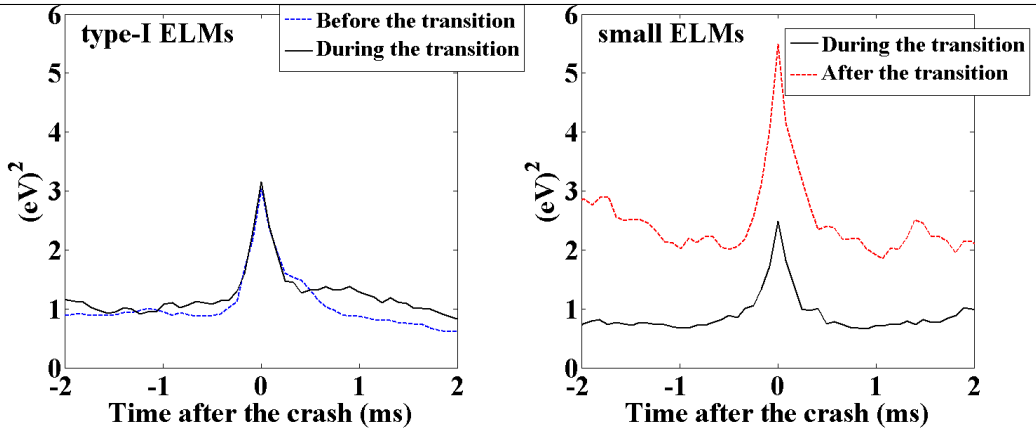

Figure 1. On the left: averaged integrated spectral power function of type-I ELMs before (black) and during (red) the transition. On the right: the same function calculated for the small ELMs, blue - before the transition, green - after. Note that the scales of the right plot are different: after the transition integrated spectral power increases ~4 times for small ELMs. On contrary, type-I ELM onsets do not change their integrated spectral power during the transition.

Considering the left plot of Fig. 1, corresponding to type-I ELMs, the maxima in both cases (before and during the transition) are the same: 100 (a. u.). Also, the duration of the type-I ELM onsets does not change over the transition. The wings of the integrated power density function give an impression of the background activity before and after type-I ELM onsets and also do not have principal differences.

The result for small ELMs is presented in Fig. 1 on the right. The peak intensity of the small ELMs after the transition is approximately four times higher than the intensity of the small ELMs before the transition (note the different y-axes). The 'wings' of the spectral power function are also much higher due to a higher level of the background fluctuations. The duration of the small ELMs does not change with the transition and is comparable with the duration of type-I ELM onsets. It is also noticeable, that before the transition small ELMs have less intensity than type-I ELM onsets.

Mode localization

Using the benefits of 2D ECEI the position of the temperature fluctuations related to type-I ELM onsets and small ELMs can be determined. Fig. 2 represents the fluctuation intensity as a function of ρ_{pol}. The maximum of the intensity in both cases, before and after the transition, is inside the separatrix and is close to $\rho_{pol} = 1$. The comparison of these plots in Fig. 2 allows to conclude, that neither type-I ELMs onsets nor small ELMs change their spatial distribution of the intensity during the transition.

Regarding the intensity, for the small ELMs after the transition it becomes significantly higher than it was before the

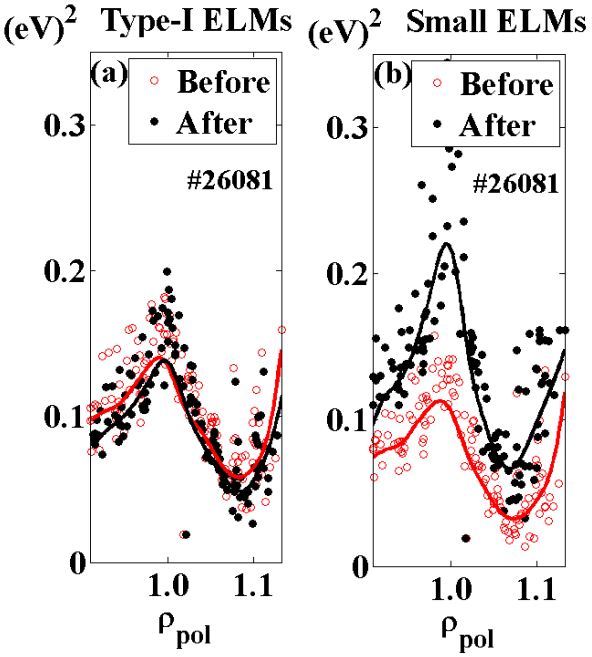

Figure 2: Mode localization. On the left for type-I ELM onsets before (in red) and during (in black) the transition. On the right for small ELMs before and after the transition. Solid lines indicate averaged profiles. As seen in 'a' and 'b', temperature fluctuations related to both type-I ELM onsets and small ELMs before as well as during the transition are localized inside the separatrix.

transition. For type-I ELM onsets it does not change significantly.

Mode velocities

2D FFT is applied to type-I ELM onsets and small ELMs to see how they change during the transition to the small ELM regime (figure 3). The inclination of the distribution in the 2D FFT plot gives information on the mode velocity (v=ω/k); as reference, the v=5 km/s line is plotted. No significant differences in the plots before and during the transition can be seen for type-I ELMs: in both plots (Fig. 3a, b) the type-I ELM onsets have the same mode velocity and the amplitude in both cases also stays the same. The inclination of the distribution correspond to a velocity around 5 km/s in electron diamagnetic drift direction. This velocity does not change during the transition.

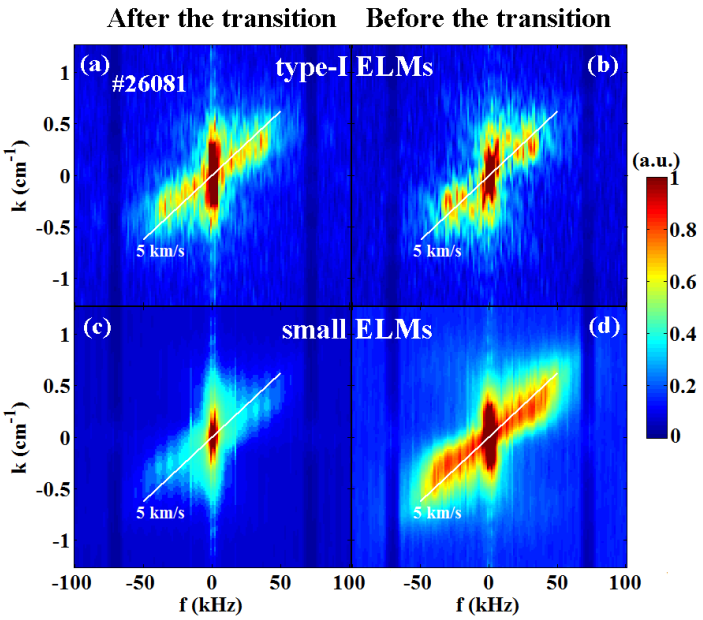

Figure 3: 2D FFT of type-I ELM onsets before (a) and during (b) the transition and of small ELMs before (c) and after (d) the transition. The inclination corresponding to the velocity of 5 km/s is marked with the white lines. The temperature fluctuations related to the small ELMs after the transition are much more pronounced than the fluctuations before.

Regarding the small ELMs, at the beginning of the transition they are weak, which is seen in the Fig. 3c: the mode distribution is very faint. In contrast, after the transition small ELMs become very well pronounced (Fig. 3d). It is noticeable, that the mode velocities for small ELMs also stay around 5 km/s.

Plasma kinetic profiles

In order to compare the conditions which trigger type-I ELMs and small ELMs, plasma temperature, density and pressure profiles are considered prior to the crash events. The time window, where the events are considered, is taken during the middle part of the transition.

As it is seen from the figure 4, type-I ELMs are triggered, on average, at higher pressures than small ELMs. Higher pressure gradient in case of type-I ELMs is caused by both a higher electron temperature and pedestal top density.

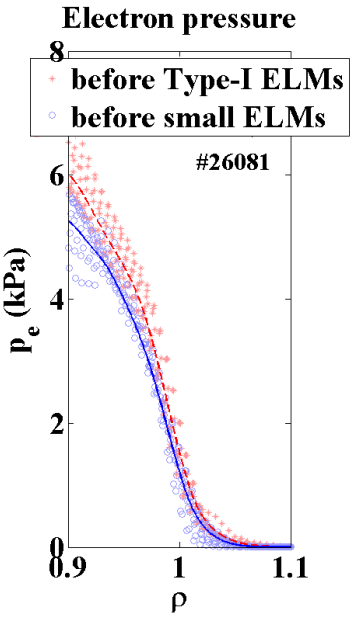

Figure 4: Plasma electron density profiles for the moments prior to type-I ELM onsets (red dots) and prior to small ELMs (blue dots). Solid lines indicate averaged profiles. Plasma profiles prior to small ELM crashes on average are below the profiles prior to type-I ELM onsets.

Discussion

Both modes are localized close to the separatrix, in the same narrow region of 2 cm, and do not change their position during the transition. The average mode velocities also do not change over the transition and is around 5 km/s in the electron diamagnetic drift direction. These similarities indicate that

type-I ELMs and small ELMs are instabilities of the same nature. The rotation velocity probably correspond to the ExB rotation of the plasma.

Type-I ELMs do not change any of the considered characteristics (localization, velocity, intensity) during the transition, apart from their frequency, which gradually reduces until they totally disappear. In contrast, small ELMs, which have already existed in the plasma before the transition, do not only increase their frequency, but also strongly start to grow in amplitude. The duration of the small ELMs does not change, which means, that the amplitude increases due to higher mode intensity. The analysis of plasma kinetic profiles indicates, that, on average, small ELMs are triggered at lower values of electron pressure gradients at the pedestal top, than type-I ELMs.

Each small ELM reduces the pressure slightly, which elongates the time needed for the kinetic profiles to recover and, thus, increases the time for the next type-I ELM to occur. This effect combined with the observation, that during the transition small ELMs change their behavior, while type-I ELMs do not, suggest an explanation for the type-I ELM mitigation mechanism. The density threshold does not affect type-I ELMs, but rather the small ELMs, destabilizing them and causing them to occur more often. As each small ELM reduces the pressure gradient, it cannot reach high enough values to trigger type-I ELMs.

References

[1] H. Zohm Plasma Phys. Control. Fusion **38** (1996) 105
[2] N. Oyama et al. Plasma Phys. Control. Fusion **48** (2006) A171
[3] I.G.J. Classen et al. Rev. Sci. Instrum. **81** (2010) 10D929
[4] J.E. Boom et al. Nucl. Fustion. **51** (2011) 103039